

SUBCRITICAL CRACKING BEHAVIOUR UNDER ENVIRONMENTS IN A LOW STRENGTH-HIGH TOUGHNESS STEEL

A. N. Kumar and R. K. Pandey

Applied Mechanics Department, Indian Institute of Technology, New Delhi-110016, India

ABSTRACT

The kinetics and mechanism of subcritical crack growth in a Ni-Cr-Mo steel quenched and tempered at 600°C, have been investigated in 3.5 per cent NaCl and H₂S impregnated acetic acid solutions. The J-integral parameter² is used to describe the cracking behaviour. The sulphide environment is found to be more aggressive than the chloride solution. The cracking process requires considerable energy dissipation, and the mechanism of crack growth is different in both the environments.

KEYWORDS

Environmental cracking, critical J values, energy dissipation, hydrogen embrittlement.

INTRODUCTION

High strength metals and alloys are known to be susceptible to subcritical cracking and premature failure in presence of aggressive environments (Thompson and Bernstein, 1979; Johnson and Willner, 1965; Landes and Wei, 1973; Carter, 1971; Stellwag and Kaesche, 1979). Hydrogen has been recognized to be the most damaging species in environment induced cracking (EIC) of high strength alloys (Thompson and Bernstein, 1979; Beachem, 1972; Hirth and Johnson, 1976). The kinetic behaviour of subcritical crack growth in these alloys has been successfully described using the LEFM approach (Johnson and Willner, 1965; Landes and Wei, 1973; Carter, 1971; Stellwag and Kaesche, 1979). However, subcritical crack growth behaviour study in low strength high toughness materials has received little attention.

The present communication is concerned with the studies of kinetics and mechanism of EIC in a low alloy steel tempered at 600°C. The alloy in this condition possesses relatively low strength and high fracture toughness and the K-approach is

invalid because of crack tip plasticity. An attempt has been made in the present work to apply the post-yield fracture parameters like the J-integral and COD to characterize the subcritical cracking behaviour in this alloy. The study has been confined to two hostile environments; namely, 3.5 percent aqueous sodium chloride solution and the hydrogen sulphide (H_2S) saturated acetic acid solution. These environments are frequently encountered in practice as in pipe lines for transportation of crude oil, components of marine vehicles, oil refineries, petrochemical industries.

EXPERIMENTAL PROCEDURE

Material and Heat Treatment

The chemical composition of the steel investigated is given in Table I. Round tensile specimens of dia. 4.1 mm, gauge length 27.0 mm and SEN fracture toughness specimens of dimensions 12 mm x 25 mm x 200 mm were machined with their lengths parallel to the rolling direction. The specimens were austenitized at $850^\circ C + 5^\circ C$ for 0.5 hr., followed by oil-quenching and liquid nitrogen treatment. The hardened specimens were tempered at $600^\circ C$ for an hour and subsequently air cooled.

TABLE I: Chemical Composition

C	Mn	P	S	Si	Ni	Cr	Mo
0.36	0.58	0.018	0.020	0.24	1.46	1.10	0.25

Experiments

Tensile properties were determined by testing the specimens in an Instron m/c. Fracture toughness values were evaluated by testing the precracked SEN specimens in three point bend using a Tensometer. Load (P) vs. load point displacement (LPD) and load vs. electrical potential (EP) plots (Fig. 1) were obtained and analyzed to get the J_{Ic} and $(COD)_c$ values corresponding to the point of crack initiation.

Precracked SEN specimens were subjected to cantilever loading for environmental study in a specially designed test jig. Fresh aqueous solutions of 3.5 per cent NaCl (pH~5.5) and the H_2S impregnated acetic acid (pH~3.0 and H_2S Concentration 1400-1500 ppm) were supplied continuously to the cracked part of the loaded specimen. The test set-up facilitated monitoring of the following during testing: (a) the onset of subcritical crack growth, (b) failure time using electrical clock system, (c) subcritical crack growth using a travelling microscope, (d) load point displacement (LPD) by LVDT, (e) crack mouth opening displacement (CMOD) with the help of a clip gauge.

J-Integral Measurement

The J-integral approach was used to describe the initiation of EIC in the steel investigated. A specimen identical to that used for environmental study was loaded in air to obtain a P - LPD plot. The J-values corresponding to various points

on the plot were calculated considering the initial crack length by using Begley-Landes approach (Begley and Landes, 1972). In presence of environments the specimens were loaded to a particular J value, J_{Ic} and the test was continued for a minimum period of 100 hrs^o. If the test failed to cause appreciable change in LPD or crack extension at the J_{Ic} level, the applied J value was increased slightly and the test was continued. The process was repeated till the specimen reached a critical J level where appreciable change in Δa or LPD was noticed. Once the specimen reached the critical J level, the changes in LPD and Δa as a function of time were recorded, maintaining the load constant.

RESULTS AND DISCUSSION

Tensile and Fracture Toughness Data

The tensile properties and the fracture toughness values of the alloy in 600 C_J tempering condition are reported in Table II. The reported $(K_{Ic})^J$ values is derived from the measured J_{Ic} value using the relation:

$$(K_{Ic})^J = [J_{Ic} \cdot E / (1 - \nu^2)]^{1/2}$$

TABLE II: Tensile and Fracture Toughness Data

Yield Strength (σ_y) MPa	Tensile Strength (MPa)	%. El	%. RA	J_{Ic-2} (kJm^{-2})	$(K_{Ic})^J$ ($MPa\sqrt{m}$)	COD_c (μm)
1029	1117	11	59	45.4	101.8	57.5

Subcritical Crack Growth

An appreciable crack extension was found to occur preceding unstable fracture in both the environments. (Figs. 2 and 3). The crack extension continued without exhibiting any constant crack growth rate region unlike many high strength materials (Johnson and Willner, 1965; Landes and Wei, 1973; Carter, 1971; Stellwag and Kaesche, 1979; Kumar, 1982). The ratios of subcritical crack extension to original crack length i.e., $\Delta a/a_o$ values were found to be 0.75 and 0.62 in NaCl and H_2S environments respectively. It is also worth mentioning here that these crack extensions in NaCl and H_2S media took place over a range of applied J level equal to 17-162 kJm^{-2} and 10-114 kJm^{-2} respectively. Thus, a greater reduction of the load bearing capacity of the alloy occurs in the H_2S medium than in NaCl solution is evident from the present work.

Threshold J Value, J_{Isc}

The P - LPD plots as obtained during loading and subcritical crack extension in the environments (Fig. 4) are analyzed to compute the J-integral values corresponding to various points on the plots using the instantaneous crack lengths. The threshold J values, J_{Isc} corresponding to the onset of subcritical cracking are J_{Isc} reported in Table III. A range of J_{Isc} values are given as a precise determination of J_{Isc} was not possible. The J_{Isc} under H_2S environment is found to be around 60 per cent of the J_{Isc} obtained in presence of

NaCl solution.

TABLE III : Threshold and Terminal J Values

Environments	J_{Isc} (kJm^{-2})	Av. J_{Isc}/J_{Ic}	J_{If} (kJm^{-2})	J_{If}/J_{Ic}
Chloride	17.6-20.3	0.42	162.5	3.6
Sulphide	10.4-11.5	0.24	114.0	2.5

Energy Dissipation During EIC

The terminal J values, J_{If} were determined from the P-LPD plots (Fig. 4) using the final crack length. The J_{If} as well as the J_{If}/J_{Ic} values are reported in Table III. Large values of J_{If} compared to J_{Ic} indicate that substantial energy dissipation is needed during EIC. Also, higher J_{If}/J_{Ic} ratio for NaCl suggested greater energy dissipation during subcritical cracking than that for H_2S medium. The energy dissipation per unit crack extension, $\Delta J/\Delta a_c$ ($\Delta J = J_{If} - J_{Isc}$) is also calculated to be 35.1 and 18.2 MJm^{-3} for the NaCl and the H_2S mediums, respectively. The requirement of larger energy for the cracking process under NaCl solution is also evident from Fig. 4 as the load had to be increased for the continuation of crack growth unlike the H_2S medium. The higher load and consequently large plastic enclave rendered the cracking process more difficult in the chloride medium. The plastic deformation was found to be much restricted under H_2S medium resulting in lesser energy dissipation.

Critical COD during EIC

The measured CMOD values during subcritical cracking in NaCl solution were converted to instantaneous crack tip COD values using the standard bend relationship (Veerman and Muller, 1972). The COD_i values are found to increase continuously with t and Δa_i the increase being more during the final stages of crack growth (Fig. 5). The critical COD value at unstable fracture, COD_{If} is found to be 250 μm .

In addition to COD_i , the variation in COD values at the original crack tip i.e. COD_T were also computed considering the original crack length, a_0 (Fig. 5). The terminal value, COD_{Tf} is measured to be 400 μm . The large difference between the COD_{Tf} and COD_c values may be attributed to the (a) change in crack length and (b) large plastic deformation associated with subcritical cracking. On the other hand, the substantial difference between COD_{If} and COD_c appears only due to crack tip rounding and blunting (Kumar, 1982).

Mechanism of Ambient vs. Environmental Fracture

The microfractographic investigation under SEM revealed that a microvoid coalescence mode of fracture is predominant in this condition of the alloy when tested in ambient condition. The fracture surfaces obtained from testing in chloride solution, however, exhibited large number of secondary cracks, deep

pits, dimples and substantial plastically deformed zones (Fig. 6). The mode of cracking is predominantly due to pitting and secondary crack formation in this environment. This study indicates that the mechanism of failure under NaCl environment is stress corrosion cracking coupled with hydrogen embrittlement. The presence of considerable amount of corrosion product (assumed to be due to anodic dissolution) on the fracture surfaces is an evidence for the contribution of SCC in inducing cracking.

The fracture surfaces formed under sulphide environment, however, were found to be characterized by the complete absence of dimples and presence of deep secondary cracks revealing intergranular type of cracking (Fig. 7). Some scattered pits and plastically deformed regions could also be noticed. The in-situ study on miniature specimens under SEM helped to reveal very fine cracks originating from the inclusions/carbides particles and their joining in the direction of stress (Kumar 1982). This indicates that the hydrogen trapping at inclusion/carbide-matrix interfaces gives rise to initiation of cracking. The recombination of atomic hydrogen is inhibited by the formation of iron sulphides and facilitates the penetration of hydrogen into the metal (Karpenko, G.V., and I.T. Vasilenko, 1979). Some of the hydrogen may precipitate as hydrogen gas molecules in the microvoids around inclusions/carbides resulting in high internal pressure within the microvoids. The EIC is believed to occur when the built up internal pressure exceeds certain limiting value. From the present work the susceptibility to EIC of the alloy in sulphide environment appears to be mainly due to hydrogen embrittlement.

CONCLUSIONS

1. J-integral approach is useful to describe the subcritical cracking behaviour in the presence of aggressive environment in low strength-high toughness steels where large plastic zone accompanies the crack growth. The alloy is susceptible to subcritical cracking in both the NaCl and H_2S media, the H_2S environment being more hostile.
2. The J_{If}/J_{Ic} ratios of about 3.6 and 2.5 for the NaCl and H_2S environments respectively, reveal that considerable energy dissipation occurs during the subcritical cracking process. The energy dissipation per unit crack extension for the NaCl medium is found to be twice than that for the H_2S medium.
3. It is believed that the hydrogen induced cracking is responsible for the crack growth under the sulphide medium whereas the stress corrosion cracking coupled with hydrogen embrittlement causes fracture under the NaCl environment.

ACKNOWLEDGEMENT

The authors express their gratitude to Prof. V. Raghavan for his interest in the present study.

REFERENCES

Beachem, C.D. (1972). *Met. Trans.*, **3**, 437-451.
 Begley, J.A., and J.D. Landes (1972). *ASTM, STP 514*, 1-11.
 Carter, C.S. (1971). *Engg. Frac. Mech.*, **3**, 1-13.
 Hirth, J.P., and H.H. Johnson (1976). *Corrosion*, **32**, 3-8.
 Johnson, H.H., and A.M. Willner (1965). *Appl. Mat. Res.*, **4**, 34-42.
 Karpenko, G.V., and I.T. Vasilenko (1979). *Stress Corrosion Cracking of Steels*, 69-93.
 Kumar, A.N. (1982). *Ambient Fracture Behaviour and Environmental Crack Growth Kinetics in a Low Alloy and a Microalloyed Steel*, Ph.D. Thesis, I.I.T., New Delhi, India, 287-295.
 Landes, J.D., and K.P. Wei (1973). *Int. J. Frac.*, **9**, 277-293.
 Stellweg, B., and H. Kaesche (1979). *Corrosion*, **35**, 39-402.
 Thompson, A.W., and I.M. Bernstein (1979). In K.W. Staehle and M.G. Fontana (eds.), *Advances in Corrosion Science and Technology*, **7**, 53-69.
 Veerman, C.C., and J. Muller (1972). *Engg. Frac. Mech.*, **4**, 25-32.

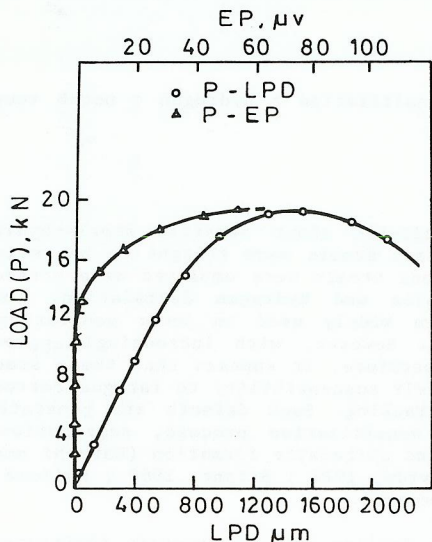


FIG-1 TYPICAL P-LPD AND P-EP PLOTS

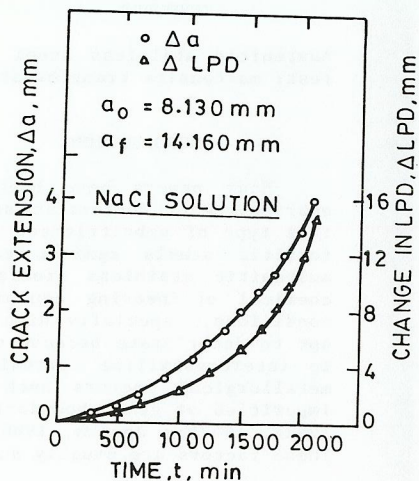


FIG-2 VARIATION OF Δa AND ΔLPD WITH TIME, t

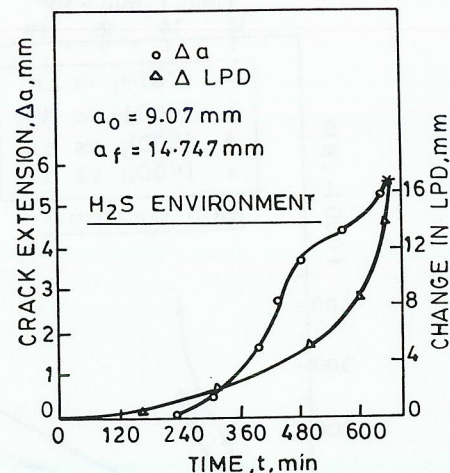


FIG-3 VARIATION OF Δa AND LPD WITH TIME, t

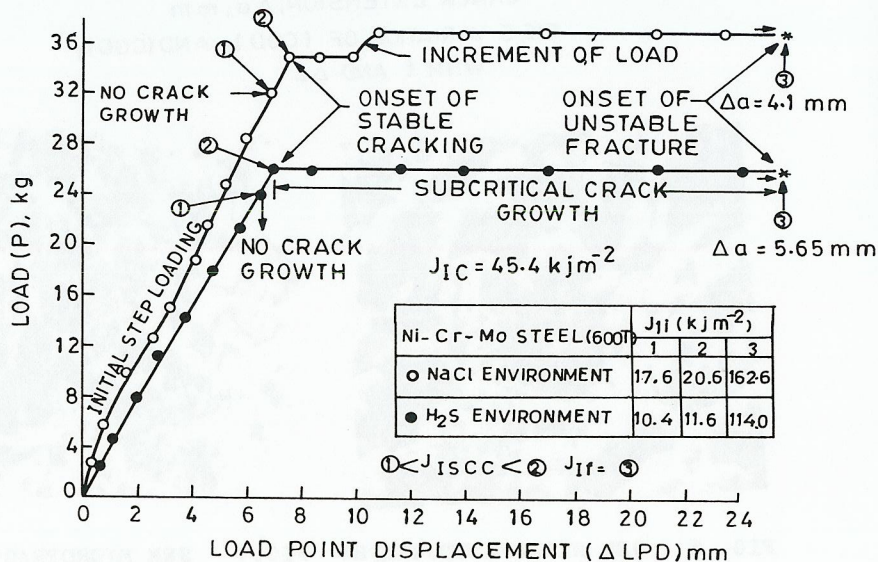


FIG-4 P-LPD PLOT FOR Ni-Cr-Mo STEEL (600T)

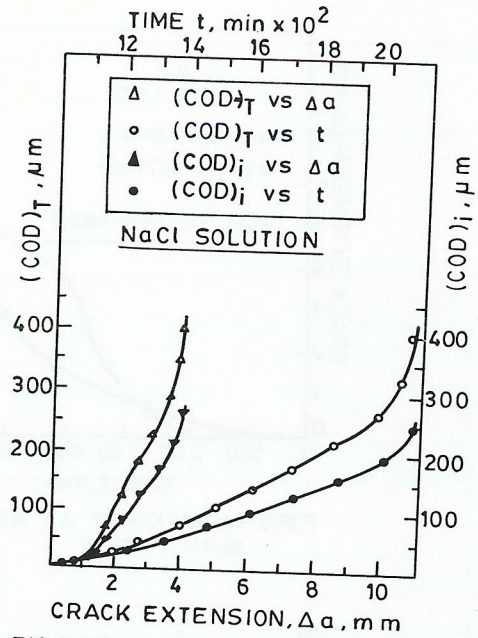


FIG.5 VARIATION OF $(COD)_i$ AND $(COD)_T$ WITH t AND Δa

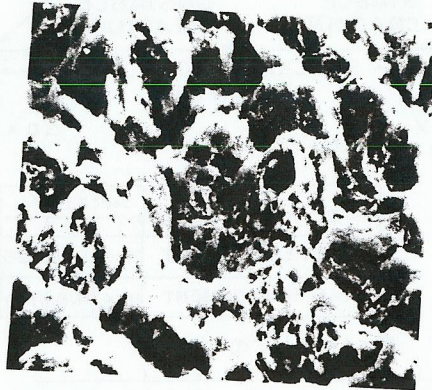


FIG. 6 SEM MICROFRACTOGRAPHS (Sodium Chloride environment, 500 X)

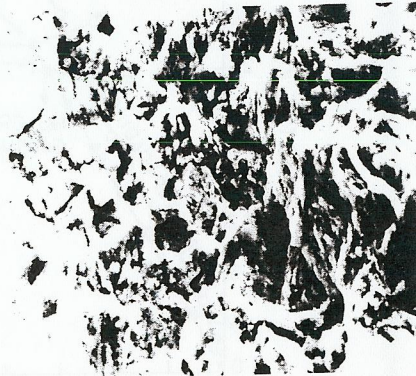


FIG.7 SEM MICROFRACTOGRAPHS (Hydrogen sulphide environment, 500 X)